Available online at www.sciencedirect.com
SCIENCE DIRECT®
Polyhedron 24 (2005) 451–461
POLYHEDRON
www.elsevier.com/locate/poly

A *N*,*N*′-diacetate benzodioxotetraazamacrocycle and its transition metal complexes

Sara Lacerda [a], Maria Paula Campello [a], Isabel C. Santos [a], Isabel Santos [a,*], Rita Delgado [b,c,*]

[a] *Departamento de Química, Instituto Tecnológico e Nuclear, Estrada Nacional, 10 Apartado 21, 2685-953 Sacavém, Portugal*
[b] *Instituto de Tecnologia Química e Biológica, UNL, Apartado 127, 2781-901 Oeiras, Portugal*
[c] *Instituto Superior Técnico, Av. Rovisco Pais, 1049-001 Lisboa, Portugal*

Received 8 November 2004; accepted 16 December 2005

Abstract

Reaction of 2,9-dioxo-1,4,7,10-tetraazabicyclo[1.10.1]hexadeca-1(11),13,15-triene-4,7-diacetic acid (**H_2L1**) with $CuCl_2 \cdot 2H_2O$ in ethanol at pH 6 led to the monomeric benzodioxochlorocomplex [Cu(**L′1**)Cl] (**1**) (**HL′1** = monoethylesther of **H_2L1**). X-ray structural analysis has shown that in complex **1** the Cu is five-coordinated by two nitrogen and two oxygen atoms of the macrocycle and by a chloride, displaying a square pyramidal coordination geometry. One of the acetate arms does not coordinate to the Cu and has suffered an in situ ethanolic esterification reaction. The protonation constants of **H_2L1** and the stability constants of its complexes with Cu^{2+}, Ni^{2+}, Zn^{2+}, Cd^{2+} and Pb^{2+} were determined by potentiometric methods and in some cases by ^{1}H NMR spectroscopy. The stability constants of the complexes follow the trend $[Ni(\mathbf{H_{-1}L1})]^- > [Cu(\mathbf{H_{-1}L1})]^- \gg [Pb(\mathbf{H_{-1}L1})]^- > [Zn(\mathbf{H_{-1}L1})]^- > [Cd(\mathbf{H_{-1}L1})]^-$, probably due to steric requirements. Spectroscopic measurements (absorption and EPR) at different pH values have shown the effect of the pH on the coordination sphere of the Cu complexes.

Keywords: Macrocycles; Monomeric Cu(II) benzodioxotetraazamacrocycle chloro complex; Stability constants; EPR of copper(II) complexes

1. Introduction

Due to their participation in a great number of important biological processes, all organisms accumulate certain levels of copper, zinc, nickel and iron, in order to survive. However, an excess of these metals is very toxic and macrocyclic polyamine ligands have been explored as possible sequestering chelators. The stability and kinetic inertness of d-transition complexes with macrocyclic polyamines, when compared with those formed with the corresponding linear ligands, make the macrocyclic polyamine complexes interesting for application in a wide variety of areas, such as catalysis, biomimicry, metallotherapy and diagnostic or therapeutic applications in Nuclear Medicine. In this specific field, copper is a very interesting d-transition element due to the large number of radionuclides with physical properties suitable for imaging (^{60}Cu, ^{61}Cu, ^{62}Cu and ^{64}Cu) or therapy (^{64}Cu and ^{67}Cu) [1].

As a part of our ongoing research work on the synthesis and characterisation of complexes with d- and f-transition metals, potentially interesting for radio diagnostic and/or radiotherapy [2–5], we have been exploring the chemistry of the previously described benzodioxotetraazamacrocyclic 2,9-dioxo-1,4,7,10-tetraazabicyclo [1.10.1] hexadeca-1(11),13,15-triene-4,7-diacetic acid (**H_2L1**) (Fig. 1) [6,7].

* Corresponding authors. Tel.: +351 21 9946201; fax: + 351 21 994 1455.
E-mail address: isantos@itn.mces.pt (I. Santos).

0277-5387/$ - see front matter © 2005 Elsevier Ltd. All rights reserved.
doi:10.1016/j.poly.2004.12.008

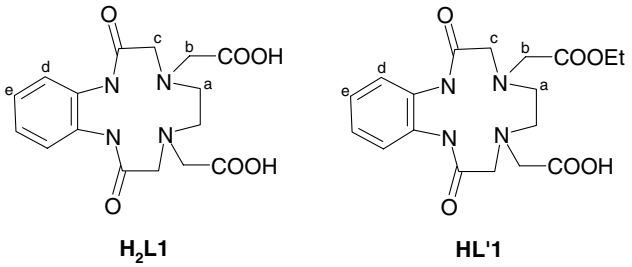

Fig. 1. 2,9-Dioxo-1,4,7,10-tetraazabicyclo[1.10.1]hexadeca-1(11),13, 15-triene-4,7-diacetic acid (**H_2L1**) and its monoethylesther (**HL′1**).

In this work, we describe the new monomeric and neutral chlorocomplex [Cu(**L′1**)Cl] (**1**) (**HL′1** = monoethylesther of **H_2L1**: 4-methylethylesther-2,9-dioxo-1,4,7, 10-tetraazabicyclo[1.10.1]hexadeca-1(11),13,15-triene-7-acetic acid ($C_{18}H_{23}N_4O_6$)). The structural differences between **1** and the dimeric Cu complex, previously described [7], led us to study more deeply the acid–base equilibrium of compound **H_2L1** as well as the stability constants of its complexes with Cu^{2+}, Ni^{2+}, Zn^{2+}, Cd^{2+} and Pb^{2+}, which will be also reported therein.

2. Experimental

2.1. Materials

Reactions were run under nitrogen atmosphere with magnetic stirring. Bulk solvent removal was done by rotary evaporation under reduced pressure and trace solvent removal from solids was done by vacuum pump. Solvents were either used as purchased or dried according to the standard literature procedures. Ethylenediaminetetraacetic dianhydride and *o*-phenylenediamine were obtained from the Aldrich Chemical Co. Copper salts were obtained from Baker's Analyzed. All reagents for synthesis and analyses were of analysis grade.

The benzodioxotetraazamacrocycle-*N*,*N*′-diacetic acid (**H_2L1**) was synthesised as previously described [6]. The purity of the compound was checked by the usual characterisation techniques.

2.1.1. Synthesis of [Cu^{II}(**L′1**)Cl] (**1**)

A solution of $CuCl_2 \cdot 2H_2O$ (0.11 g, 0.651 mmol in 2 cm^3 of ethanol) was added to a solution of **H_2L1** (0.237 g, 0.651 mmol in 8 cm^3 of ethanol). The resulting brown mixture was refluxed for 2 h. After cooling to room temperature, the solution was filtered through diatomaceous earth and washed with methanol. X-ray-quality green single crystals were obtained by slow diffusion of methanol. *Anal.* Calc. for $C_{18}H_{23}ClCuN_4O_6.H_2O$: C, 42.44; H, 5.14; N, 11.00. Found: C, 42.45; H, 4.63; N, 11.02%. UV: 704 nm (54 mol^{-1} dm^3 cm^{-1}), 382 nm (133 mol^{-1} dm^3 cm^{-1}).

2.2. X-ray crystal analyses

Suitable green crystals ($0.25 \times 0.20 \times 0.06$ mm) were mounted in air on a goniometer head. Data were collected at room temperature with the crystal mounted in a glass capillary. An Enraf-Nonius CAD4 diffractometer equipped with graphite monochromatised Mo Kα radiation ($\lambda = 0.71069$ Å) in the ω–2θ scan was used for measurements. Lorentz, polarisation effects and empirical absorption correction based on psi-scans [8] were applied to the collected intensities.

The structure was solved by direct methods using SIR97 [9] and refined by full-matrix least-squares on F^2 methods using the program SHELXL97 [10] and the WINGX software package [11]. All non-hydrogen atoms were refined anisotropically. Hydrogen atoms were placed in calculated positions. Molecular graphics were prepared with Ortep3 [12].

The crystal data and structure refinement details for **1**: Empirical formula, $C_{18}H_{23}N_4O_6ClCu$; $M = 490.39$ g mol^{-1}; Orthorhombic, $P2_12_12_1$, $a = 10.6410(13)$, $b = 13.0690(16)$, $c = 14.505(2)$ Å, $V = 2017.2(4)$ $Å^3$, $Z = 4$, $D_{calc} = 1.615$ g cm^{-3}, $\mu = 1.260$ mm^{-1}, $F(0\,0\,0) = 1012$; 271 parameters, no restraints, 2372 unique reflections measured, of which 2216 observed [$I > 2\sigma(I)$], $R_1 = 0.0624$, $wR_{all} = 0.1130$, Highest peak and deepest hole 0.574 and −0.282 e A^{-3}, θ range: 2.37–25.97°, Limiting indices, $-13 \leqslant h \leqslant 13$, $0 \leqslant k \leqslant 16$, $-17 \leqslant l \leqslant 0$, Goodness-of-fit = 1.061.

2.3. Spectroscopic studies

^1H and ^{13}C NMR spectra were recorded with a Bruker AMX-300 spectrometer at probe temperature in D_2O, using 3-(trimethylsilyl)-propanoic acid-*d*4-sodium salt as internal reference in the ^1H and dioxane in the ^{13}C spectra.

Electronic spectra were measured with a Cary 500 Version 8.01 spectrophotometer using aqueous solutions $\approx 1 \times 10^{-3}$ mol dm^{-3} of the copper complexes and $\approx 2 \times 10^{-3}$ mol dm^{-3} of the nickel complexes, at different pH values: ≈3, ≈6 and 10 for copper and ≈4, ≈8 and ≈11 for nickel complexes. The choice of the pH values was based on the species distribution diagram for each metal, selecting the maximum pH of formation of the species: [ML], $[M(H_{-1}L)]_-$ and $[M(H_{-2}L)]_{2-}$.

EPR spectroscopic measurements of the copper complex were recorded with a Bruker ESP 380 spectrometer equipped with continuous-flow cryostats for liquid nitrogen, operating at X-band. The complexes ($\approx 2 \times 10^{-3}$ mol dm^{-3} in 1:1 DMSO:H_2O solution) were prepared at pH 3.51, 6.37 and 10.26 and were recorded at 96 K. The EPR spectrum of a 1:1 DMSO/H_2O solution of **1** (at pH 3.23) was also recorded.

2.4. Potentiometric measurements

2.4.1. Reagents and solutions

Metal ion solutions were prepared at about 2.5×10^{-3} mol dm^{-3} from the nitrate salts of the metals and were titrated using standard methods [13]. Deionised (Millipore/Milli-Q System) distilled water was used. Carbonate-free solutions of the KOH titrant were obtained, maintained and discarded when the percentage of carbonate was about 0.5% of the total amount of base [14].

2.4.2. Equipment and work conditions

The equipment was used as described before [2–4,15]. The temperature was kept at 25.0 ± 0.1 °C, atmospheric CO_2 was excluded from the cell during the titrations by passing purified nitrogen across the top of the experimental solution in the reaction cell. The ionic strength of the solutions was kept at 0.10 mol dm^{-3} with KNO_3.

2.4.3. Measurements

The $[H^+]$ of the solutions was determined by the measurement of the electromotive force (emf) of the cell, $E = E^{\circ\prime} + Q\log[H^+] + E_j$. $E^{\circ\prime}$, Q, E_j and $K_w = ([H^+][OH^-])$ were obtained as described previously [2–4,15]. The term pH is defined as $-\log[H^+]$. The value of K_w was found equal to $10^{-13.80}$ $(\text{mol dm}^{-3})^2$. The potentiometric equilibrium measurements were made on 20.00 cm^3 of $\approx 2.00 \times 10^{-3}$ mol dm^{-3} ligand solutions diluted to a final volume of 25.00 cm^3, in the absence of metal ions and in the presence of each metal ion for which the C_M:C_L ratio was 1:1. A minimum of two replicate measurements was taken.

The emf data were taken after additions of 0.050 cm^3 increments of standard KOH solution, and after stabilisation in this direction, equilibrium was then approached from the other direction adding standard nitric acid.

In the cases of copper (II) and nickel (II), the degree of complex formation of the metal complexes was too high to prevent the use of the direct potentiometric method. Metal–metal competition titration methods were used. Lead (II) and cadmium (II) were the second metals used, respectively.

2.4.4. Calculation of equilibrium constants

Protonation constants $K_i^H = [H_iL]/[H_{i-1}L][H]$ were calculated by fitting the potentiometric data for the free ligand to the HYPERQUAD program [16]. Stability constants of the various species formed in solution were obtained from the experimental data corresponding to the titration of solutions of different ratios of the ligand and metal ions, also with the aid of the HYPERQUAD program. The initial computations were obtained in the form of overall stability constants or $\beta_{M_mH_hL_l}$ values:

$$\beta_{M_mH_hL_l} = \frac{[M_mH_hL_l]}{[M]^m[L]^l[H]^h}.$$

The hydrolysis constants of the metal ions were taken from the literature and kept constant for the calculations [17].

For ligand **H$_2$L1**, the first protonation constant was determined by ^{1}H NMR titration, due to its high value. For this determination, a solution of **H$_2$L1** (≈0.01 mol dm^{-3}) was prepared in D_2O and the pD was adjusted by addition of DCl or CO_2-free KOD with an Orion 420A instrument fitted with a combined Ingold 405M3 microelectrode. The $-\log[D^+]$ was measured directly in the NMR tube, after the calibration of the microelectrode with buffered aqueous solutions. The final pD was calculated from pD = pH* + (0.40 ± 0.02), where pH* corresponds to the reading of the pH meter [18,19].

3. Results and discussion

The benzodioxotetraazamacrocycle **H$_2$L1** has been synthesised and characterised as previously described [6]. Reaction of **H$_2$L1** with $CuCl_2 \cdot 2H_2O$ in ethanol, at pH 6 in 1:1 (Cu: **H$_2$L1**) molar ratio, resulted in a brown solution, upon refluxing for 2 h. This solution was filtered at room temperature and a small portion of methanol added. Slow diffusion of MeOH led to green monocrystals suitable for X-ray crystallographic analysis. By X-ray diffraction analysis, the complex formed was formulated as [Cu(**L′1**)Cl] (**1**). This is a monomeric Cu^{2+} complex anchored by a modified benzodioxotetraazamacrocycle. In complex **1**, the Cu is five-coordinated by two nitrogen atoms of the macrocyclic backbone, two oxygen atoms, one from one amide group and the other from an acetate arm, and a chloride atom occupies the fifth position. The second acetate arm of the macrocycle does not coordinate to the Cu and it has experienced an in situ ethanolic esterification reaction. The ORTEP drawing of **1** is shown in Fig. 2, and selected bond lengths and angles are listed in Table 1.

The Cu(II) centre displays a five-coordination environment, which can be described as a square pyramidal polyhedron (SP). The basal plane is defined by the N(3), O(2), O(5) and the chloride atoms, while the apical position is occupied by the N(4) atom.

Most of the Cu(II) five-coordinate complexes known display either distorted square pyramidal (SP) or distorted trigonal bipyramidal (TBP) coordination geometries. To evaluate the degree of distortion from the ideal polyhedron mainly two methods have been developed. The simplest method, which can be applied when there is an apical bond distance longer then the others, is based on the ratio of the two basal angles of the square plane, which is given by the expression $\tau = [(\theta - \phi)/$

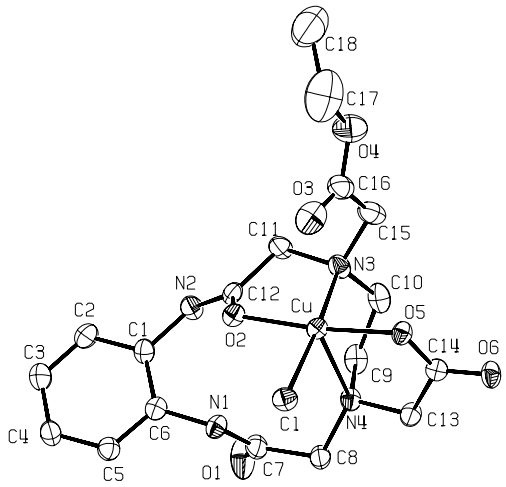

Fig. 2. ORTEP view of the complex **1**; thermal ellipsoids are drawn at 40% probability level.

Table 1
Selected bond lengths (Å) and angles (°) for **1**

Bond lengths			
Cu–O(5)	1.942(4)	O(2)–C(12)	1.265(7)
Cu–O(2)	1.964(4)	O(5)–C(14)	1.264(8)
Cu–N(3)	2.100(6)	O(6)–C(14)	1.225(8)
Cu–N(4)	2.420(5)	O(3)–C(16)	1.246(9)
Cu–Cl	2.2540(19)	O(1)–C(7)	1.220(8)
O(2)–C(12)	1.258(6)	O(4)–C(16)	1.319(10)
Bond angles			
O(5)–Cu–O(2)	172.66(18)	Cl–Cu–N(4)	96.17(14)
O(5)–Cu–N(3)	89.30(17)	C(13)–N(4)–C(9)	111.1(5)
O(2)–Cu–N(3)	83.60(17)	C(13)–N(4)–C(8)	107.4(5)
O(5)–Cu–Cl	96.10(14)	C(9)–N(4)–C(8)	111.9(5)
O(2)–Cu–Cl	91.12(13)	C(13)–N(4)–Cu	99.3(3)
N(3)–Cu–Cl	173.54(17)	C(9)–N(4)–Cu	100.7(4)
O(5)–Cu–N(4)	81.25(18)	C(8)–N(4)–Cu	125.6(4)
O(2)–Cu–N(4)	99.27(17)	C(12)–O(2)–Cu	112.2(4)
N(4)–Cu–N(3)	81.10(18)	C(14)–O(5)–Cu	119.7(4)

60] × 100 (%), being $\tau = 0$ for an ideal SP and $\tau = 100$ for an ideal TBP coordination geometries [20]. For complex **1**, the angles considered were Cl–Cu–N(3) and O(2)–Cu–O(5), and the value calculated for τ was 1.46%. The square plane is folded along the axis defined by Cl, Cu and N(3), yielding a dihedral angle between the planes [Cl, N(3), O(5)] and [O(2), Cl, N(3)] of 5.65(23)°. The angle between basal plane and the apical line Cu–N(4) is 78.91(15)°. The copper is 0.0217(24) Å above the basal plane and the apical N(4) atom is 2.348(6) Å below this plane, yielding a Cu–N(4) apical bond distance of 2.420(4) Å, which is longer than the copper nitrogen bond distance in the basal plane (Cu–N(3), 2.100(6) Å). The dihedral angle between the aromatic ring and the plane defined by the nitrogen atoms of the macrocyclic backbone is 14.45(30)°, being the copper atom 1.6750(31) Å above this plane. The Cu–N(3) bond distance is in the expected range of 1.99–2.08 Å, normally found for five-coordinated Cu(II) complexes stabilised by amines [20a, 21].

In complex **1**, the Cu–O(2) and Cu–O(5) bond lengths are 1.964(4) and 1.942(4) Å, respectively. As in other five-coordinated Cu(II) complexes, the bond Cu–O_{amide} is slightly longer than Cu–$O_{carboxylate}$. The Cu–Cl bond length of 2.254(2) Å in **1** is in the expected range [22].

The formation of the monomeric complex **1**, described herein, is certainly related with the reaction conditions used for the synthesis and recrystallisation of this complex (1:1 **H_2L1**:$CuCl_2 \cdot 2H_2O$, pH 6, ethanol, 2 h reflux, slow diffusion of MeOH), which certainly were also responsible for the in situ sterification of one carboxylic acid arm. In fact, a dimer copper complex, isolated by Fernando and co-workers [7], has been obtained by reacting **H_2L1** with $CuCl_2 \cdot 2H_2O$ in basic aqueous conditions and monocrystals were formed by the slow concentration of this solution. In the dimer, the Cu atom is six-coordinated by two oxygen atoms of the carboxylate arms, an oxygen from an amide group and two nitrogen atoms from the macrocyclic backbone; the sixth coordination position being occupied by an oxygen atom of a carboxylate arm from an adjacent molecule.

Taking into account that different complexes can be formed using different reaction conditions and also the potential interest of copper for biological applications, we decided to study the coordination chemistry of this ligand, including the determination of the stability constants of **H_2L1** with Cu and also with other metals, such as Ni, Zn, Cd and Pb, which also have biological interest, due to their high toxicity. Spectroscopic measurements were also performed in order to understand the structure of some of the complexes in aqueous solution.

3.1. Acid–base behaviour

The acid–base behaviour of compound **H_2L1** has been studied by potentiometry and by ^{1}H NMR spectroscopy. Only four protonation constants were determined. From the remaining two constants, one is very high (corresponding to the amide centre) and the other very low to be determined. Indeed, in our work conditions only one amide centre can be deprotonated, and even this one at very high pH values, then the corresponding constant was determined by ^{1}H NMR spectroscopy. The protonation constants of **H_2L1** are shown in Table 2 as well the values published in literature for other related tetraazamacrocyclic ligands shown in Fig. 3.

Taking into account the structure of **H_2L1**, results published in the literature and our ^{1}H NMR data (see below), the values in Table 2 indicate that the first protonation occurs at one amide nitrogen atom, as already mentioned. The second constant corresponds to the protonation of an amine nitrogen, which in spite of being a low value it is the usual number found for

Table 2
Protonation constants (log units) for **H_2L1** and other similar ligands

Overall protonation constants [stepwise constants]	**H_2L1**[a]	**H_2L1**[b]	**H_2L2**[c,d]	**H_2L3**[c,d]
$\beta_1^H[k_1^H]$	12.81(20) [12.81]			
$\beta_2^H[k_2^H]$	18.84(1) [6.03]	6.07 [6.07]	6.50 [6.50]	6.41 [6.41]
$\beta_3^H[k_3^H]$	22.24(1) [3.40]	9.34 [3.27]	10.04 [3.54]	9.81 [3.40]
$\beta_4^H[k_4^H]$	24.35(3) [2.11]			

[a] This work, 25.0 °C, $I = 0.10$ mol dm^{-3} KNO_3, values in parentheses are standard deviations in the last significant figures.
[b] 25 °C, $I = 0.1$ mol dm^{-3} KCl, [7].
[c] 25 °C, $I = 0.1$ mol dm^{-3} KCl, [23,24].
[d] The β values shown were calculated based on the stepwise stability constants given by the authors.

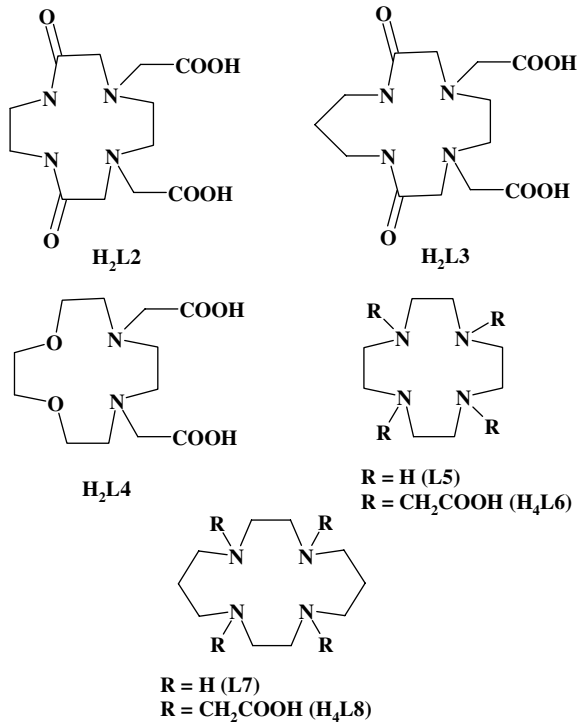

Fig. 3. Tetraazamacrocyclic ligands related with **H_2L1**: **H_2L2** (2,9-dioxo-1,4,7,10-tetraazacyclododecane-4,7-diacetic acid), **H_2L3** (2,9-dioxo-1,4,7,10-tetraaza-cyclotridecane-4,7-diacetic acid), **H_2L4** (1,4-dioxa-7,10-diazacyclododecane-7,10-diacetic acid), **L5** (1,4,7,10-tetraazacyclododecane; cyclen), **H_4L6** (1,4,7,10-tetraazacyclododecane-1,4,7,10-tetraacetic acid; dota), **L7** (1,4,8,11-tetraazacyclotetradecane; cyclam), **H_4L8** (1,4,8,11-tetraazacyclotetradecane-1,4,8,11-tetraacetic acid; teta).

the protonation of amine centres in close proximity of one electron-withdrawing amide group [25,26]. The third constant corresponds to the protonation of the acetate arm bound to the non-protonated amine nitrogen [25] and finally, the fourth constant can be attributed to the protonation of the remaining amine nitrogen or the remaining acetate or both simultaneously.

The first determined protonation constant is so high that only could be determined by ^{1}H NMR titration in the pD range 8–15, Fig. 4.

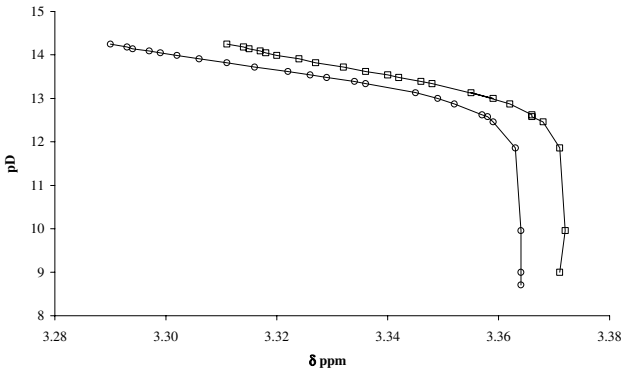

Fig. 4. ^{1}H NMR titration curves of **H_2L1**: proton H_b (○) and proton H_c (□).

The ^{1}H NMR spectra of compound **H_2L1** exhibit four resonances for the entire pD range. At high pD values, the spectra show two multiplets assigned to the aromatic protons (H_d and H_e) and two singlets, integrating for four and two protons, assigned to the H_b, H_c and H_a, respectively. At low pD values, the spectra show only one multiplet resonance for the four aromatic protons (H_d/H_e) and three singlets of equal intensity (2H) for the H_a, H_b and H_c protons.

The variation of chemical shifts (δ) of the H_b and H_c protons in function of pD values were used to determine the first protonation constant. As can be seen in Fig. 4, the δ are downfield shifted when the pD value increases. The shifts are small, because the centre to be protonated is far from H_b or H_c, but significant enough to be used for calculations. Based on these data, two pK_D values were determined independently, converted in pK_H, and the final pK_H given by the average of these. The conversion of the pK_D values in pK_H was made using the correlation pK_D = 0.11 + 1.10pK_H determined for polyaza and polyoxa-polyaza macrocyclic compounds by Delgado et al. [18]. The average pK_H value found was 12.81(4). However if all the experimental errors for the determination of this value were taken into account a standard deviation of about 0.2 should be indicated as more realistic.

The values determined in this work (see Table 2) for the second and the third stepwise protonation constants are comparable to the values previously reported by Cathala et al. [6] and Fernando and co-workers [7]. It was possible to determine the protonation constant of one amide centre for **H_2L1**, and not in the case of **H_2L2** and **H_2L3** and many other similar cyclic amide complexones studied by Fernando and co-workers [23,24,26], due to the presence of the benzene ring in **H_2L1** that turn the adjacent amide more acidic. However, the inclusion of this constant, and also the fourth one, led to an overall basicity for **H_2L1**, which is about 15 log units higher than the previously described value with the consequent repercussions on the stability constant values of its metal complexes.

Potentiometric studies of **H_2L1** with Cu^{2+}, Ni^{2+}, Zn^{2+}, Cd^{2+} and Pb^{2+} were performed also at 25.0 °C and 0.10 M ionic strength in KNO_3, in order to determine the corresponding stability constant. The values found are shown in Table 3, together with those taken from literature for the related **H_2L2** and **H_2L3** macrocycles.

Only mononuclear species were formed with the studied metal ions, namely $[M(\mathbf{H_{-1}L1})]^-$, $[M\mathbf{L1}]$ and $[M(\mathbf{H_{-2}L1})]^{2-}$. The $[M(\mathbf{HL1})]^+$ species only appears with Ni^{2+}, while $[M(\mathbf{H_{-3}L1})]^{3-}$ is formed with Cu^{2+} and Cd^{2+}.

At physiological pH, the $[M(\mathbf{H_{-1}L1})]^-$ complex is formed at about 100% for Cu^{2+} and Ni^{2+}, while for Pb^{2+} and Zn^{2+} this species is the main complex only at pH $\geqslant$ 9, and for Cd^{2+} the amount of $[Cd(\mathbf{H_{-1}L1})]^-$ formed is low at physiological pH, being $[M\mathbf{L1}]$ always present. This information suggests that Ni^{2+} and Cu^{2+} easily deprotonate the first amide centre, while the other studied metal ions only manage to do it at higher pH values. Even though the thermodynamic stability constants do not give structural information, being impossible to ascribe the acid–base reactions that occur at high pH values to amide deprotonation or to the hydrolysis of water molecules directly coordinated to the metal centre. Based in these experiments is also impossible to realize if a structural arrangement occurs upon deprotonation of the amide centre for the nickel and copper complexes. However a slow reaction occurs after the deprotonation of the first amide centre for the case of nickel, because it was found completely different potentiometric curves when the solution containing the metal and ligand in a 1:1 ratio is titrated with base (formation of complexes) or with acid upon the complete formation of complexes which clearly suggests a structural rearrangement (supplementary material).

The Ni(II) complex $[M(\mathbf{H_{-1}L1})]^-$ exhibits the highest thermodynamic stability constant followed by Cu(II) being the corresponding values significantly lower for

Table 3
Stability constants (log units) for complexes of **H_2L1** and other related ligands with several divalent metal ions (charges were ignored)

Ion	Equilibrium quotient	**H_2L1**[a]	**H_2L1**[b]	**H_2L2**[c,d]	**H_2L3**[c,d]
Ni^{2+}	$[ML]/[M]\times[L]$	17.73(8)	9.4	11.27	10.08
	$[M(HL)]/[M]\times[H]\times[L]$	22.81(3)		12.82	11.68
	$[M(H_2L)]/[M]\times[H]^2\times[L]$	27.04(6)			
	$[M(H_{-1}L)]/[M]\times[H]^{-1}\times[L]$	8.76(5)	2.5	1.97	−0.60
	$[M(H_{-2}L)]/[M]\times[H]^{-2}\times[L]$			−11.93	−10.38
Cu^{2+}	$[ML]/[M]\times[L]$	17.13(5)	9.04	11.34	10.46
	$[M(HL)]/[M]\times[H]\times[L]$	21.72(4)		12.63	11.55
	$[M(H_{-1}L)]/[M]\times[H]^{-1}\times[L]$	8.54(6)	4.51	4.04	3.08
	$[M(H_{-2}L)]/[M]\times[H]^{-2}\times[L]$	−2.70(7)	−4.33	−6.37	−2.97
Zn^{2+}	$[ML]/[M]\times[L]$	13.23(4)	7.56	8.98	9.13
	$[M(HL)]/[M]\times[H]\times[L]$	20.40(2)		10.45	11.49
	$[M(H_{-1}L)]/[M]\times[H]^{-1}\times[L]$	2.68(6)	0.42	−0.58	−0.84
	$[M(H_{-2}L)]/[M]\times[H]^{-2}\times[L]$		−10.84	−12.52	−12.08
Cd^{2+}	$[ML]/[M]\times[L]$	12.68(5)		7.3	7.4
	$[M(HL)]/[M]\times[L]\times[H]$	19.84(2)		9.9	9.6
	$[M(H_{-1}L)]/[M]\times[H]^{-1}\times[L]$	2.48(6)		−3.1	−3.2
	$[M(H_{-2}L)]/[M]\times[H]^{-2}\times[L]$	−9.42(4)		−15.4	−15.2
Pb^{2+}	$[ML]/[M]\times[L]$	13.43(2)			
	$[M(HL)]/[M]\times[H]\times[L]$	20.88(1)			
	$[M(H_{-1}L)]/[M]\times[H]^{-1}\times[L]$	3.60(3)			

[a] This work; 25.0 °C, $I = 0.10$ mol dm^{-3} KNO_3, **L** is $\mathbf{H_{-1}L1}^{3-}$, the resulting species upon three successive deprotonation reactions of **H_2L1**, including the deprotonation of one amide group, see text; values in parentheses are standard deviations in the last significant figures.
[b] 25 °C, $I = 0.1$ mol dm^{-3} KCl, [7].
[c] 25 °C, $I = 0.1$ mol dm^{-3} KCl, [23,24].
[d] The β values shown were calculated based on the stepwise stability constants given by the authors.

the other three metal ions, Pb, Zn and Cd. The trend $[Ni(\mathbf{H_{-1}L1})]^- > [Cu(\mathbf{H_{-1}L1})]^- \gg [Pb(\mathbf{H_{-1}L1})]^- > [Zn(\mathbf{H_{-1}L1})]^- > [Cd(\mathbf{H_{-1}L1})]^-$ does not follow the usual Irving–Williams order of stability [27]. However, analogous trends have already been reported. In general, steric requirements of the ligands on complex formation (macrocyclic type or other) or coordination geometry preferences are on the basis of the inversion of stability for the nickel and copper complexes [28].

The stability constant values of **H_2L1** with all the metals studied are higher than the previously reported [7], which is expected on the basis of the different protonation values presented. The direct comparison of values of this work and the previously reported ones can be made by the calculation of pM ($-\log[M^{2+}]$) values. In Table 4 are shown the pM values for the different complexes together with those calculated from the potentiometric data for other related ligands (see Fig. 3), at physiological pH [29]. The pCu and pZn values for **H_2L1** calculated using our stability constants are identical, but the pNi is higher, than the reported ones.

The discrepancy found for Ni probably results from the very high value of its stability constant added to its slow kinetic formation. Indeed this constant, as well as that for the copper complex, was determined by a competition reaction (see Section 2) because the complex is completely formed at the beginning of the titration, this means at very low pH values, see Fig. 5. The ligand **H_2L3** presents lower pM values when compared with those of **H_2L1**, except for zinc. The lower values for **H_2L3** are expected due to the larger cavity size of this macrocycle, although the high value presented for Zn is not expected. The pM values for **H_2L1** and **H_2L2** are very similar suggesting that the introduction of the benzene ring into the framework of **H_2L1** has a minor influence on complex formation, or that the donor atoms involved in the coordination to the metal are not specially affected by the presence of the benzene ring.

Table 4
pM ($-\log[M^{2+}]$)[d] values determined for metal complexes of **H_2L1** at physiological pH

Ion	**H_2L1**[a]	**H_2L1**[b]	**H_2L2**[c]	**H_2L3**[c]
Ni^{2+}	12.32	9.99	11.67	10.04
Cu^{2+}	11.73	11.91	11.64	11.83
Zn^{2+}	8.00	7.99	8.93	9.09
Cd^{2+}	7.45		7.88	7.90
Pb^{2+}	8.33			

[a] This work.
[b] Ref. [7].
[c] Ref. [23,24].
[d] The values were calculated for 100% excess of free ligand, using the program HYSS [29], $C_L = 2C_M = 1 \times 10^{-5}$ mol dm^{-3}, and the stability constants given in Table 2.

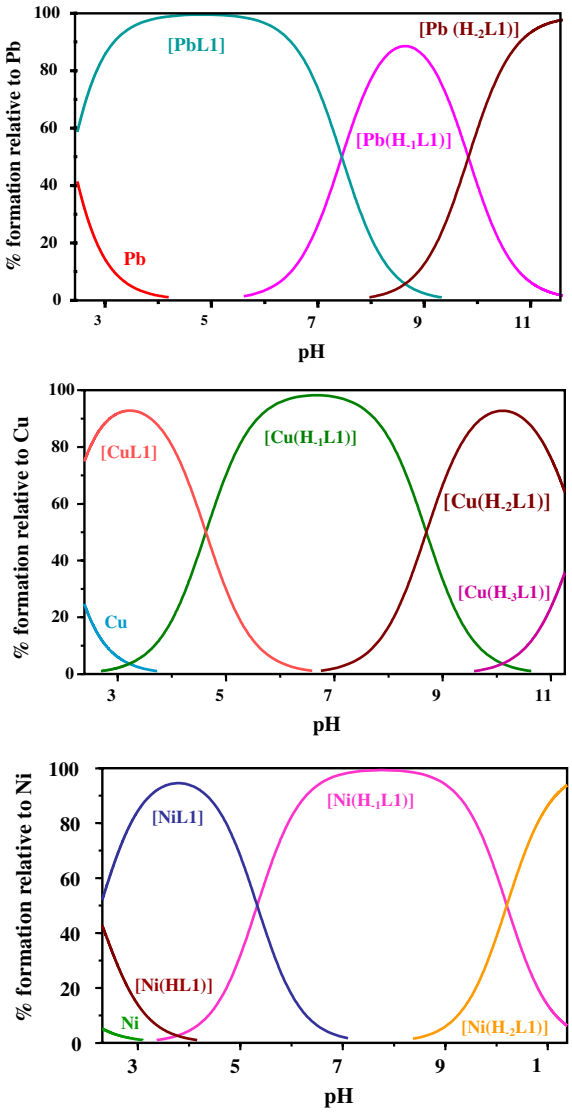

Fig. 5. Species-distribution diagrams for the Pb^{2+}, Cu^{2+} and Ni^{2+} complexes with **H_2L1** in water, $C_L = C_M = 4.201 \times 10^{-5}$ mol dm^{-3}.

3.2. Spectroscopic studies in solution

The UV–Vis-near IR spectra of the Ni(II) and the Cu(II) complexes, and the X-band EPR spectra of the Cu(II) ones were recorded at pH values of about 3, 6.5 and 10 for the copper complexes and about 4, 8 and 11 for the nickel ones. The selected pH values correspond to the maximum percentage of [M**L**], $[M(\mathbf{H_{-1}L})]^-$ and $[M(\mathbf{H_{-2}L})]^{2-}$ species, respectively, with minimum percentage of the other species present, as shown on the species distribution diagrams, see Fig. 5.

3.3. UV–Vis-near IR spectra

The electronic spectra of the Ni/**H_2L1** complexes exhibit at all pH values three main bands typical of distorted octahedral or square pyramidal geometries: one

in the range 1008–952 nm (broadband), the second in the range 597–562 nm and the third at about 380 nm, (Table 5). The spectra were recorded upon full stabilisation (about 18 h) of solutions at each pH. Indeed the slow kinetics, already verified in the potentiometric measurements, was confirmed, the final spectra displaying important differences in number of bands and absorption maxima from those recorded immediately upon preparation.

The visible and especially the near-IR bands shift to higher energies (of about 50 nm for the first and 35 nm for the second one), when the pH increases from 3.76 to 11.39. The observed blue shift indicates an increase of the ligand field, suggesting the coordination of an additional donor atom to the metal centre. The increase of the molar absorptivity accounts to a more distorted geometry of the complex.

The electronic spectra of the copper complexes are not especially informative about the adopted geometry in solution, however the band in the near-IR region points to a distorted geometry, and the blue shifts of the visible band with the increase of the pH were also observed, see Table 5. However, a faster kinetics of formation of the copper complex in comparison with that of nickel was noted, as already mentioned above.

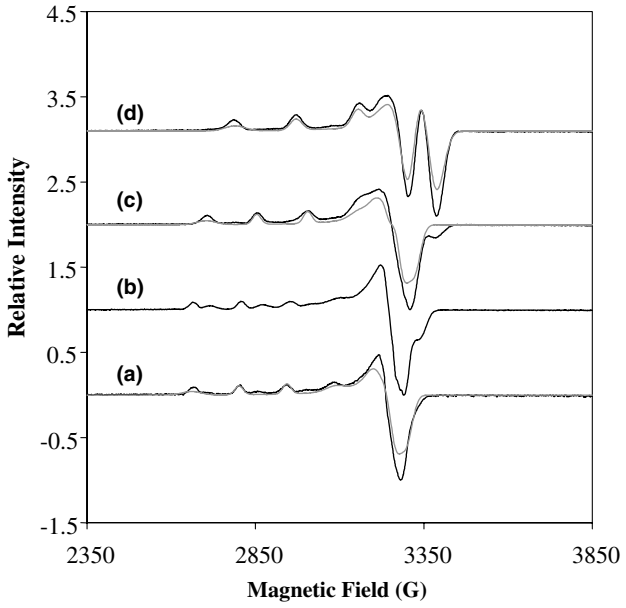

Fig. 6. X-band EPR spectra of copper complexes of **H_2L1** in $\approx 2 \times 10^{-3}$ mol dm^{-3} and 1:1 H_2O/DMSO solutions (black lines) and its simulated spectra (grey lines) at different pH values: (a) pH 3.51; (b) pH 6.37 and (c) pH 10.26. The spectrum of a solution of **1** in 1:1 H_2O/DMSO (pH 3.23) is also shown (d). All the spectra were recorded at 96 K, microwave power of 2.0 mW and modulation amplitude of 1 mT. The frequency was 9.405, 9.407, 9.408 and 9.407 GHz, respectively.

3.4. EPR spectroscopy of copper complexes

The EPR spectra of copper complexes in solution at different pH indicated the presence of only one species, while the EPR spectrum of the solution obtained by dissolving the crystals of **1** in DMSO/H_2O indicated the presence of two species, see Fig. 6. All spectra showed the expected four well-resolved lines at low field, due to the interaction of the unpaired electron spin with the copper nucleus. The hyperfine coupling constants (A) and g values obtained by the simulation of the spectra [30] are shown in Table 6, together with those of other copper (II) complexes taken from literature for comparison. The simulation of the spectra indicates three different g values with $g_z > (g_x + g_y)/2$ and the lowest $g \geqslant 2.04$, which is characteristic of mononuclear copper (II) complexes having rhombic-octahedral with elongation of the axial bonds or distorted square-based pyramidal symmetries, and $d_{x^2-y^2}$ ground state.

At the three pH studied, the complexes have g_z and A_z parameters consistent with different type of donor atoms close lying the metal. At pH 3.51, these parameters are consistent with N_2O_2 equatorial coordination sphere [31]. The differences between them can be visualised in the diagram g_z versus A_z presented in Fig. 7, and rationalised in terms of different axial field for each complex. Indeed, the g_i and A_i values are related to the electronic transitions by the factors derived from the ligand-field theory [32,33]: the g_i values increase

Table 5
Spectroscopic UV–Vis-near IR data for the Ni^{2+} and Cu^{2+} complexes of **H_2L1** at several pH values in aqueous solution and 25 °C

Complex	pH	λ/nm (ε/mol^{-1} dm^3 cm^{-1})
Ni^{2+}/H_2L1	3.76	1008 (27), 597 (8), 375 (19)
	8.02	1151 (28), 1036 (sh., 26), 959 (30), 842 (sh., 20), 595 (20), 363 (sh., 34), 339 (sh., 40)
	11.39	1147 (27), 1017(sh., 31), 952 (39), 850 (sh., 30), 562 (24), 342 (sh., 65)
Cu^{2+}/H_2L1	3.51	752 (65), 487 (sh., 24), 382 (69)
	6.63	1020 (sh., 22), 670 (61), 444 (sh., 60), 375 (450)
	10.10	643 (sh., 160), 560 (186), 384 (197)
1[a]	3.23	704 (54), 382 (133)

[a] Crystals of **1** dissolved in aqueous solution.

Table 6
Spectroscopic EPR parameters for the copper (II) complexes of **H_2L1** and other related ligands taken from literature ($A_i \times 10^4$ cm^{-1})

Ligand/complex (pH)		g_x	g_y	g_z	A_x	A_y	A_z
H_2L1 (3.51)[a]		2.060	2.088	2.338	1.7	7.9	155.1
H_2L1 (6.37)[a]		2.050	2.080	2.293	3.1	12.8	161.4
H_2L1 (10.26)[a]		2.039	2.064	2.194	2.5	13.5	186.8
1 (3.23)[a]	**A**	2.060	2.088	2.336	1.4	6.4	153.6
	B	2.050	2.081	2.293	2.5	11.9	163.8
H_2L1 (6.6)[b]		2.035	2.090	2.290			165.1
H_2L1 (12.0)[b]		2.040		2.195			190.2
H_2L3 (<7)[c]		2.039	2.073	2.336			147.0
H_2L3 (>7)[c]		≈2.0		2.190			188.0
H_2L4 [d]		2.045	2.073	2.251	5.4	16.6	187.8
L5 [e]		2.057		2.198	24.1		184.2
L7[e]		2.049		2.186	38.7		205.0
H_4L6[e]		2.062		2.300			150.3
H_4L8[e]		2.050		2.249			168.0
Cu(H_2O)$_6$[f]		2.08		2.4			134.0

[a] This work.
[b] Ref. [7].
[c] Ref. [23].
[d] Ref. [36a].
[e] Ref. [36b,36c].
[f] Ref. [36d].

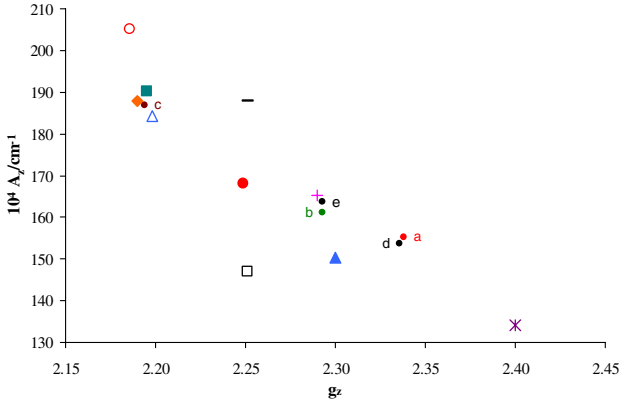

Fig. 7. Diagram A_z vs. g_z EPR parameters for the copper (II) complexes studied (×) and others from literature formed with the following ligands: ● **a** **H_2L1** (pH 3.51), ● **b** **H_2L1** (pH 6.37), ● **c** **H_2L1** (pH 10.26), ● **d** **1** (specie A), ● **e** **1** (specie B), + **H_2L1** (pH 6.6) [7], ■ **H_2L1** (pH 12) [7], ◆ **H_2L3** (pH > 7) [23], □ **H_2L3** (pH < 7) [23], – **H_2L4** [36a], ○ **L7** [36b,36c], △ **L5** [36b,36c], ▲ **H_4L6** [36b,36c], ● **H_4L8** [36b,36c] and ⁎ Cu(H_2O)$_6$ [36d].

and the A_i values decrease as the equatorial ligand field becomes weaker or stronger the axial ligand field and this occurs with the simultaneous red-shift of the d–d absorption bands in the electronic spectra (see Tables 5 and 6) [33–35]. Herein, when the pH increases a blue-shift is observed, and simultaneously the g_z decrease and the A_z values increase, which is consistent with the increase of the equatorial field. These features are also consistent with the potentiometric results, which have shown that the deprotonation of one amide nitrogen atom occurs at pH ~ 6.

The EPR spectrum of crystals of **1** showed that two species are present in different proportions. The g_z and A_z parameters suggest that the crystals of **1** in solution have a different structure than in the solid state, as the chloride atom is probably replaced by an oxygen of a water molecule. The resulting parameters are consistent with a mixture of the spectrum of **H_2L1** at pH 3.51 (specie A) and of **H_2L1** at pH 6.37 (specie B), being the first in a higher proportion (about 75%). This suggests that an equilibrium between the two corresponding structures is responsible by the observed EPR spectrum.

The A_z versus g_z diagram shown in Fig. 7, together with the known geometries of some of the complexes taken from the literature [36], allow the following considerations: (1) the right region of the diagram, having higher g_z and lower A_z values, is occupied by complexes with oxygen atoms in the equatorial plane, such as Cu(H_2O)$_6$ (⁎); (2) in the middle region of the diagram complexes with octahedral geometry are found, having the four nitrogen atoms of the macrocycle forming the equatorial plane and oxygen atoms in the axial positions (● **H_4L8**); (3) the complexes having four nitrogen atoms of the macrocyclic ring at the equatorial plane are located in the left part of the diagram and exhibit square-planar (○ **L7**) or square pyramidal (△ **L5**) geometries. The parameters of the copper complexes of **H_2L1** change considerably with the increase of the pH, with the decrease of g_z, the increase of A_z and a corresponding blue shift, accounting a stronger equatorial ligand field. Indeed, at pH 3.5 these parameters are consistent with a N_2O_2 coordination sphere, while those for the complexes at pH ≈ 6 and ≈10 point to arrangements with stronger equatorial ligand fields, in agreement to the presence of an increased number of nitrogen as donor atoms.

4. Concluding remarks

Although **H_2L1** was reported before, the present study allowed to extend the knowledge of its behaviour and of its metal complexes in solution and in the solid state. Our potentiometric and ^1H NMR studies revealed that the deprotonation of one of the amides occurs at a pH lower than usual due to the presence of the benzene ring into the macrocyclic backbone, allowing its determination. It was also verified that the nickel complex has a thermodynamic stability higher than the copper one, and therefore the usual Irving–Williams trend of stability is not found, probably due to steric strain imposed by the ligand.

By reacting **H_2L1** with $[CuCl_2] \cdot 2H_2O$, in EtOH at pH 6 and using the 1:1 M/L molar ratio, the monomeric complex **1** was obtained. This complex is quite different from the dimeric Cu^{2+} complex isolated previously by Fernando and co-workers [7].

Based on the electronic data, it was possible to predict that at low pH values (pH 3.51) two amine nitrogen atoms and two oxygen atoms from the acetate arms or from the amides of the framework are involved in the coordination sphere of the Cu, as the EPR parameters are consistent with a N_2O_2 donor atoms close lying the metal [31] and the X-ray structure of **1** also suggests. At higher pH values (about 6), the EPR parameters are consistent with a N_3O equatorial coordination sphere for the copper, in agreement also with the blue shift of the band in the visible region. This means that the deprotonation of the amide of the macrocyclic backbone, which occurs in this pH range, leads to a rearrangement of the complex with the repositioning of the Cu atom towards the centre of the macrocycle for the coordination to this amide nitrogen. This probably also happens with the nickel complex, and in this case the rearrangement is kinetically slow, as observed by our potentiometric and UV–Vis results. At high pH values is impossible to predict, based only on our potentiometric experiments, if the deprotonation of the second amide of the macrocycle occurs or if the proton that is titrated in this region derive from the hydrolysis of a water molecule directly coordinated to the metal ion. However, the EPR spectra showed unambiguously that, at least for the copper complex, the increase of the strength of the equatorial ligand field at high pH can only be ascribed to the contribution of the fourth nitrogen of the macrocycle on the metal coordination.

Acknowledgements

The authors acknowledge the financial support from Fundação para a Ciência e a Tecnologia (FCT) and POCTI, with co participation of the European Community fund FEDER (Project No. POCTI/CBO/35859/99). COST D18 is also acknowledged.

Appendix A. Supplementary data

Supplementary data associated with this article can be found, in the online version, at doi:10.1016/j.poly.2004.12.008.

Crystallographic data (excluding structure factors) for the structure of compound **1** have been deposited with the Cambridge Crystallographic Data Centre as supplementary publication no. CCDC-254663. Copies of the data can be obtained free of charge on application to CCDC, 12 Union Road, Cambridge CB2 1EZ, UK [Fax: int. code +44 1223/336 033; E-mail: deposit@ccdc.cam.ac.uk, or www: http://www.ccdc.cam.ac.uk].

References

[1] (a) J. Costamagna, G. Ferraudi, B. Matsuhiro, M. Campos, J. Canales, M. Villagrán, J. Vargas, M.J. Aguirre, Chem. Rev. 196 (2000) 125;
(b) C.J. Anderson, M.A. Green, Y. Fujibayashi, in: M.J. Welch, C.S. Redvanly (Eds.), Handbook of Radiopharmaceuticals: Radiochemistry and Applications, Wiley, New York, 2003, p. 401.
[2] P. Antunes, P.M. Campello, R. Delgado, M.G.B. Drew, V. Félix, I. Santos, J. Chem. Soc., Dalton Trans. (2003) 1852.
[3] K.P. Guerra, R. Delgado, L.M.P. Lima, M.G.B. Drew, V. Félix, J. Chem. Soc., Dalton Trans. (2004) 1812.
[4] F. Marques, K.P. Guerra, L. Gano, J. Costa, M.P. Campello, L.M.P. Lima, R. Delgado, I. Santos, J. Biol. Inorg. Chem. 9 (2004) 859.
[5] I. Santos, A. Paulo, J.D.G. Correia, Topics in Current Chemistry, vol. 252, Springer, Berlin, 2004, p. 45.
[6] B. Cathala, C. Picard, L. Cazaux, P. Tisnès, M. Momtchev, Tetrahedron 51 (1995) 1245.
[7] M.B. Inoue, L. Machi, I.C. Muñoz, S. Rojas-Rivas, M. Inoue, Q. Fernando, Inorg. Chim. Acta 324 (2001) 73.
[8] PSISCANS. A.C.T. North, D.C. Phillips, F.S. Mathews, Acta Crystallogr., Sect. A 24 (1968) 351.
[9] SIR97. A. Altomare, M.C. Burla, M. Camalli, G.L. Cascarano, C. Giacovazzo, A. Guagliardi, A.G.G. Moliterni, G. Polidori, R. Spagna, J. Appl. Crystallogr. 32 (1999) 115.
[10] SHELX97. G.M. Scheldrick, Programs for Crystal Structure Analysis (Release 97-2), Institüt für Anorganische Chemie der Universität, Tammanstrasse 4, D-3400 Göttingen, Germany, 1998.
[11] WINGX. L.J. Farrugia, J. Appl. Crystallogr. 32 (1999) 837.
[12] L.J. Farrugia, J. Appl. Crystallogr. 30 (1997) 565.
[13] G. Shwardzenbach, W. Flaschka, Complexometric Titrations, Methuen & Co, London, 1969.
[14] G. Shwardzenbach, W. Biedermann, Helv. Chim. Acta 31 (1948) 331.
[15] (a) J. Costa, R. Delgado, M.G.B. Drew, V. Félix, A. Saint-Maurice, J. Chem. Soc., Dalton Trans. 12 (2000) 1907;
(b) J. Costa, R. Delgado, M.G.B. Drew, V. Félix, R.T. Henriques, J.C. Waerenborgh, J. Chem. Soc., Dalton Trans. 18 (1999) 3253.
[16] P. Gans, A. Sabatini, A. Vacca, Talanta 43 (1996) 1739.

[17] NIST Standard Reference Database 46. NIST Critically Selected Stability Constants of Metal Complexes Database. Version 5.0. Data collected and selected by R.M. Smith and A.E. Martell, US Department of Commerce, National Institute of Standards and Technology, Washington, DC, 1998.
[18] R. Delgado, J.J.R.F. da Silva, M.T.S. Amorim, M.F. Cabral, S. Chaves, J. Costa, Anal. Chim. Acta 245 (1991) 271.
[19] A.K. Covington, M. Paabo, R.A. Robison, R.G. Bates, Anal. Chem. 40 (1968) 700.
[20] (a) G.A. McLachlan, G.D. Fallon, R.L. Martin, L. Spiccia, Inorg. Chem. 34 (1995) 254;
(b) A.W. Addison, T. Nageswara Rao, J. Reedijk, J. van Rijn, G.C. Verschoor, J. Chem. Soc., Dalton Trans. (1984) 1349.
[21] S.-G. Kang, K. Ryu, J. Kim, Bull. Kor. Chem. Soc. 19 (1998) 1005.
[22] M. Gupta, P. Mathur, R.J. Butcher, Inorg. Chem. 40 (2001) 878.
[23] M.B. Inoue, P. Oram, G. Andreu-de-Riquer, M. Inoue, P. Borbat, A. Raitsimring, Q. Fernando, Inorg. Chem. 34 (1995) 3528.
[24] M.B. Inoue, P. Oram, M. Inoue, Q. Fernando, Inorg. Chim. Acta 246 (1996) 401.
[25] R. Delgado, M.F. Cabral, R. Castanheira, A. Zhang, R. Herrmann, Polyhedron 21 (2002) 2265.
[26] (a) M.B. Inoue, I.C. Muñoz, L. Machi, M. Inoue, Q. Fernando, Inorg. Chim. Acta 311 (2000) 50;
(b) M.B. Inoue, E.F. Velazquez, F. Medrano, K.L. Ochoa, J.C. Galvez, M. Inoue, Q. Fernando, Inorg. Chem. 37 (1998) 4070.
[27] H. Irving, R.J.P.J. Williams, J. Chem. Soc. (1953) 3192.
[28] (a) R. Yang, L.J. Zompa, Inorg. Chem. 15 (1976) 1499;
(b) L.J. Zompa, Inorg. Chem. 17 (1978) 2531;
(c) R.D. Hancock, V.J. Thöm, J. Am. Chem. Soc. 104 (1982) 291;
(d) V.J. Thöm, J.C.A. Boeyens, G.J. McDougall, R.D. Hancock, J. Am. Chem. Soc. 106 (1984) 3198;
(e) D.-Y. Kong, Y.-Y. Xie, Polyhedron 19 (2000) 1527;
(f) M. Sandow, B.L. May, C.J. Easton, S.F. Lincoln, Aust. J. Chem. 53 (2000) 149;
(g) A.V. Bordunov, J.S. Bradshaw, X. Zhang, N.K. Dalley, X. Kou, R.M. Izatt, Inorg. Chem. 35 (1996) 7229;
(h) S.E. Livingstone, E.A. Sullivan, Aust. J. Chem. 22 (1969) 1363;
(i) S. Murakam, J. Inorg. Nucl. Chem. 43 (1981) 335.
[29] L. Alderighi, P. Gans, A. Ienco, D. Peters, A. Sabatini, A. Vacca, Coord. Chem. Rev. 184 (1999) 311.
[30] F. Neese, Diploma Thesis, University of Konstanz, Germany, 1993.
[31] J. Peisach, W.E. Blumberg, Arch. Biochem. Biophys. 165 (1974) 691.
[32] H.R. Gersmann, J.D. Swalen, J. Chem. Phys. 36 (1962) 3221.
[33] P.W. Lau, W.C. Lin, J. Inorg. Nucl. Chem. 37 (1975) 2389.
[34] A.W. Addison, M. Carpenter, L.K.-M. Lau, M. Wicholas, Inorg. Chem. 17 (1978) 1545.
[35] M.J. Maroney, N.J. Rose, Inorg. Chem. 23 (1984) 2252.
[36] (a) S. Chaves, A. Cerva, R. Delgado, Polyhedron 17 (1998) 93;
(b) M.C. Styka, R.C. Smierciak, E.L. Blinn, R.E. DeSimone, J.V. Passariello, Inorg. Chem. 17 (1978) 82;
(c) K. Miyoshi, H. Tanaka, E. Kimura, S. Tsuboyama, S. Murata, H. Shimizu, K. Ishizu, Inorg. Chim. Acta 78 (1983) 23;
(d) E.I. Solomon, K.W. Penfield, D.E. Wilcox, Struct. Bond. 53 (1983) 1.